HYDROLOGICAL PROCESSES
Hydrol. Process. **27**, 1959–1972 (2013)
Published online 23 May 2012 in Wiley Online Library
(wileyonlinelibrary.com) DOI: 10.1002/hyp.9304

Controls of streamflow generation in small catchments across the snow–rain transition in the Southern Sierra Nevada, California

Fengjing Liu,[1,2]* Carolyn Hunsaker[3] and Roger C. Bales[1]

[1] *Sierra Nevada Research Institute, University of California, Merced, CA, USA*
[2] *Department of Agriculture and Environmental Science and Cooperative Research Programs, Lincoln University of Missouri, Jefferson City, MO, USA*
[3] *Pacific Southwest Research Station, USDA Forest Service, Fresno, CA, USA*

Abstract:

Processes controlling streamflow generation were determined using geochemical tracers for water years 2004–2007 at eight headwater catchments at the Kings River Experimental Watersheds in southern Sierra Nevada. Four catchments are snow-dominated, and four receive a mix of rain and snow. Results of diagnostic tools of mixing models indicate that Ca^{2+}, Mg^{2+}, K^{+} and Cl^{-} behaved conservatively in the streamflow at all catchments, reflecting mixing of three endmembers. Using endmember mixing analysis, the endmembers were determined to be snowmelt runoff (including rain on snow), subsurface flow and fall storm runoff. In seven of the eight catchments, streamflow was dominated by subsurface flow, with an average relative contribution (% of streamflow discharge) greater than 60%. Snowmelt runoff contributed less than 40%, and fall storm runoff less than 7% on average. Streamflow peaked 2–4 weeks earlier at mixed rain–snow than snow-dominated catchments, but relative endmember contributions were not significantly different between the two groups of catchments. Both soil water in the unsaturated zone and regional groundwater were not significant contributors to streamflow. The contributions of snowmelt runoff and subsurface flow, when expressed as discharge, were linearly correlated with streamflow discharge (R^2 of 0.85–0.99). These results suggest that subsurface flow is generated from the soil–bedrock interface through preferential pathways and is not very sensitive to snow–rain proportions. Thus, a declining of the snow–rain ratio under a warming climate should not systematically affect the processes controlling the streamflow generation at these catchments. Copyright © 2012 John Wiley & Sons, Ltd.

KEY WORDS streamflow generation; snow–rain transition; endmember mixing analysis; southern Sierra Nevada

Received 29 January 2011; Accepted 6 March 2012

INTRODUCTION

Precipitation has been changing in volume, intensity and form (e.g. rain and snow) throughout many regions of the world because of climate warming (Dore, 2005; IPCC, 2007). In the mountains of the western United States, trends toward less precipitation falling as snow (e.g. Cayan *et al*., 2001; Mote *et al*., 2005; Knowles *et al*., 2006) and the melting of snow earlier in the year (e.g. Stewart *et al*., 2004; Bales *et al*., 2006; Rauscher *et al*., 2008) are expected to continue. The 1 April snow depth at index sites has decreased by 20%–40% since the 1950s at moderate elevations (1500–2200 m) in Sierra Nevada (Mote *et al*., 2005). Observations and modelling results have shown that less snow and earlier snowmelt lead to a shift in peak river runoff toward late winter and early spring, away from summer when water demand is highest (e.g. Barnett *et al*., 2005; Stewart *et al*., 2005). However, it is still unclear how the decline in snow relative to rain systematically affects subsurface water storage and streamflow generation (e.g. Stewart *et al*., 2005; Kundzewicz *et al*., 2007). This hydrologic insight is critical for water resource management and has important implications for water supplies at local to global scales.

The mechanisms of streamflow generation have been well studied for both rain-dominated and snow-dominated catchments across a wide range of climate, geology and vegetation. Many studies have shown that shallow subsurface flow, including lateral flow, lateral subsurface flow, through flow and interflow, is usually one of the important pathways in streamflow generation in small, forested catchments, regardless of snow or rain dominance (e.g. Hogan and Blum, 2003; Beighley *et al*., 2005; Tromp-van Meerveld and McDonnell, 2006; Redding and Devito, 2010). For example, a few studies from an 870-m^2 ponderosa pine hillslope at Los Alamos have indicated that lateral subsurface flow is an important flow process that controls snowmelt runoff at hillslope scales in semiarid environments (Wilcox *et al*., 1997; Newman *et al*., 1998, 2004). The importance of this process at catchment scales in semiarid regions with a seasonal snow cover has also been recognized (McNamara *et al*., 2005; Liu *et al*., 2008a, b; Frisbee *et al*., 2011). However, notably lacking from these studies is a direct comparison to examine how the response of subsurface flow to snow and rain differs across catchments in the same region with similar geology, vegetation and soil. A mixed snow–rain *versus* snow-dominated catchments in a given area may imply less in-catchment seasonal storage, shorter in-catchment residence

*Correspondence to: Fengjing Liu, Department of Agriculture and Environmental Science and Cooperative Research Programs, Lincoln University, 904 Chestnut Street, Jefferson City, MO 65101, USA.
E-mail: liuf@lincolnu.edu

times and earlier seasonal change of soil storage (Bales *et al.*, 2011; Hunsaker *et al.*, 2012). These discrepancies may cause differences in the processes that control streamflow generation in those catchments.

The objectives of the study reported here were to quantitatively determine the dominant processes controlling streamflow across snow-dominated and rain-dominated headwater catchments and to understand how changes in the snow–rain proportion affect streamflow generation.

METHODS

Research area

This study was conducted in eight forested catchments that make up the Kings River Experimental Watersheds, a watershed-level, integrated ecosystem project for long-term research on nested headwater streams in the southern Sierra Nevada (Figure 1). The Kings River Experimental Watersheds is operated by the Forest Service's Pacific Southwest Research Station. Four catchments are located at the Providence site, and four catchments are located at the Bull site within the Sierra National Forest, northeast of Fresno, California (Figure 1). The four catchments at the Providence site range in size from 0.49 to 1.32 km^2 and in elevation from 1479 to 2113 m, whereas the four catchments at the Bull site range in size from 0.53 to 2.28 km^2 and in elevation from 2055 to 2490 m (Table I).

Table I. Catchment characteristics

Catchment name	Area (km^2)	Elevation (m)			Mean Slope, % of rise
		Mean	Minimum	Maximum	
Providence					
P301	0.99	1979	1803	2113	19.9
P303	1.32	1900	1727	2017	22.9
P304	0.49	1882	1755	1979	23.0
D102	1.21	1754	1479	1981	32.8
Bull					
B201	0.53	2259	2150	2382	21.3
B203	1.38	2377	2195	2488	20.2
B204	1.67	2365	2192	2490	19.8
T003	2.28	2293	2055	2465	26.7

Annual precipitation was 75–90% snow in the high-elevation Bull catchments (water years 2004 to 2007) and was up to 80% rain in the lower-elevation Providence catchments (Hunsaker *et al.*, 2012). For the same period, mean air temperatures were 7.8 and 6.8 °C at the lower-Providence and upper-Bull meteorological stations, respectively. Soils are well drained, mixed, frigid Dystric Xeropsamment, formed from decomposed granite (Dahlgren *et al.*, 1997), including Shaver and Gerle–Cagwin soil at the Providence catchments and Cagwin soils at the Bull catchments (Giger and Schmitt, 1993). Litter depth and depth to bedrock vary across the

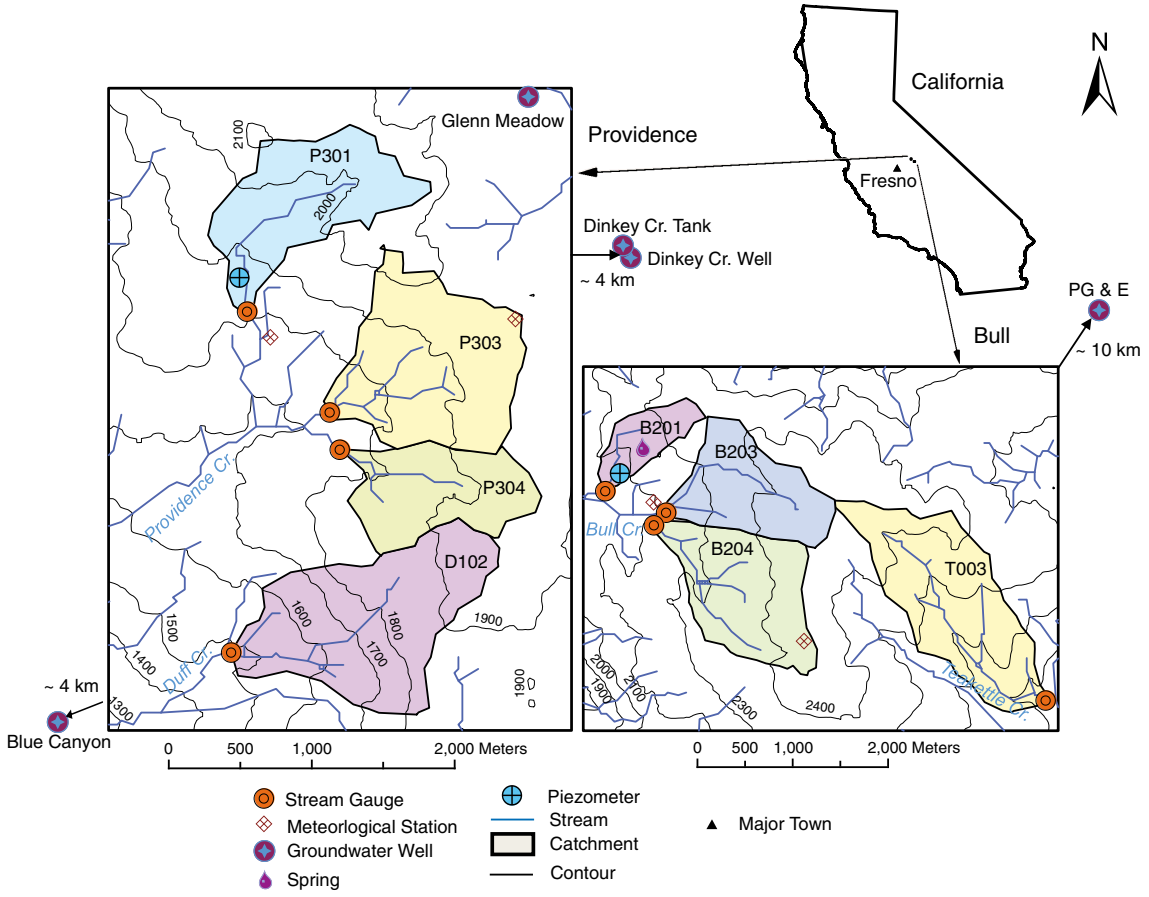

Figure 1. Study area, showing locations of eight catchments, stream gauges (stream sampling sites), meteorological stations (snowmelt sampling sites), piezometers, wells and springs. Most groundwater wells are located outside the map and indicated by directions and distances

study area, but all soils have similar texture and water percolation rate (Bales *et al*., 2011). The Providence catchments are largely mixed conifer forest, with some chaparral, barren and meadow. The Bull catchments also are mainly mixed conifer forests, with a higher proportion of red fir at higher elevations.

The study area and its vicinity are made up of granitic, metamorphic and volcanic rocks, with some glacial-till materials. Clay mineralogy is dominated by hydroxyl-Al interlayered vermiculite and gibbsite, as a result of the weathering of feldspar and plagioclase under intense leaching environment (Dahlgren *et al*., 1997). This weathering process may cause much higher cationic concentrations (e.g. Ca^{2+}, Mg^{2+} and Na^{+}) in subsurface water than in rainwater and snowmelt. This weathering environment is also very effective at removing Si in spite of the cold soil temperatures, resulting in Si-depleted minerals. Quantitative pit and surface soil samples indicated that the higher-elevation Bull watersheds had significantly greater C, N and B contents in soils but lower extractable P, Ca^{2+}, Mg^{2+} and Na^{+} contents than the lower-elevation Providence watersheds (Johnson *et al*., 2011).

Sample collection and analysis

Streamflow samples were collected biweekly at the outlets of the eight catchments from fall 2003 to fall 2007 (Figure 1). Samples were either grabbed by hand or collected by automated ISCO samplers to increase sampling frequency during a storm. The ISCO samplers were triggered when streamflow discharge exceeded a certain value and provided samples several hours apart during storm events.

Soil water was collected from Prenart samplers at two depths, 13 and 26 cm. Prenart soil samplers are suction-cup lysimeters that are made of porous teflon mixed with silica flour or stainless steel powder (for more information, refer to http://www.prenart.dk/sampler.php). Each pair of samplers was placed symmetrically at 2, 4 and 6 m away from the tree trunk, but under the canopy, and one in the open at each depth. Prenart samplers were deployed at all Providence catchments.

Snowmelt was collected using plastic sampling bottles placed at four meteorological stations (Figure 1). Each bottle has a funnel to gather snow and allow meltwater to flow into the bottle. Bottles were placed before a significant storm came and collected right after the storm ended.

Samples were also collected in 2008 and 2009 from piezometers, spring and groundwater wells in several locations (Figure 1). Groundwater was collected from drinking-water wells at Glen Meadow, Dinkey Creek, the Pacific Gas and Energy (PG & E) work centre, and the Blue Canyon Work Center two to three times in August 2008 and October 2009. A sample collected from a tank (used for supplying drinking water to local residents) near Dinkey Creek was actually from a nearby well. Samples were taken once in October 2009 from a spring at B201 and two 1.5-m depth soil piezometers at B201 and P301 meadows.

Samples collected from wells, the spring and piezometers in 2008–2009 were analyzed for major cations (Ca^{2+}, Mg^{2+}, Na^{+}, K^{+}) and anions (Cl^{-}, NO_3^{-}, SO_4^{2-}) using a Dionex 2000 Ion Chromatograph (IC) at the Environmental Analytical Laboratory of the University of California, Merced. Analytical precision (1σ standard deviation) for all ions was less than 1%, and detection limit less than $1\ \mu eq\ l^{-1}$. All other samples were analyzed for major cations and anions by using IC at the Pacific Southwest Research Station, Riverside, CA. Precision is also less than 1% for ionic concentrations. Acid neutralizing capacity (ANC) was calculated as the difference between the total concentrations of cations and anions, all in $\mu eq\ l^{-1}$.

Endmember mixing analysis and diagnostic tools of mixing models

Contributions of endmembers to streamflow were determined using tracer-based endmember mixing analysis (EMMA) in combination with the diagnostic tools of mixing models (DTMM), following Liu *et al*. (2008a). DTMM, developed by Hooper (2003), is used (i) to identify solutes that undergo chemical processes within and en route to streams and that behave conservatively upon mixing of various sources of water (endmembers) and (ii) to determine the number of endmembers needed for the mixing of conservative solutes. DTMM distinguishes whether solute correlations are controlled by chemical equilibria that are nonlinear (solute concentrations are associated with each other through polynomial functions) and mixing that is linear (solute concentrations are associated with each other by a linear function under one or more dimensions in *U*-space). Principal component analysis (PCA) is used to test which solutes are not associated linearly and which ones are, and under how many *U*-space dimensions. Those solutes with polynomial relationships indicate the predominance of a chemical reaction in their formation. Those with linear relationships suggest that their concentrations in the streamflow are a mixture of various endmembers. The number of *U*-space dimensions for the linear expressions of conservative solutes is one less than the number of endmembers needed for the mixing.

EMMA was then used with the determined conservative tracers to identify endmembers and quantify the contributions of endmembers to streamflow, following Christophersen and Hooper (1992) and Liu *et al*. (2004). PCA was performed again to extract eigenvectors by using a correlation matrix (not the original ionic concentrations) of conservative tracers (not all solutes as used in the DTMM) that were determined using DTMM. The PCA scores were used to solve for endmember contributions, a procedure mathematically the same as using two tracers for a three-component mixing model (e.g. Rice and Hornberger, 1998).

Three criteria were used to identify eligible endmembers from potential ones, following Liu *et al*. (2008a). First, eligible endmembers must form a convex polygon (e.g. a triangle in the case of three endmembers) to bind most, if not all, streamflow samples. Second, the distance of all eligible endmembers between original compositions (*S*-space) and *U*-space orthogonal projections should be reasonably short for all tracers used in the analysis. The threshold values are not available in literature, but in the past studies of Liu *et al*. (2004,

2008a, b), endmembers with the relative distances (% of the measured ionic concentrations) less than 50%–60% for all tracers worked very well, except for fresh snow with very low ionic concentrations. Third, streamflow chemistry must be well recreated for conservative tracers by using the results of EMMA.

RESULTS

Hydrology and meteorology

Annual precipitation measured at four meteorological stations along an elevation gradient of 1750 to 2463 m was essentially the same (Figure 2A). Annual mean precipitation was 95, 178, 198 and 76 cm in water years 2004, 2005, 2006 and 2007, respectively. Precipitation primarily occurred from December to March, as seen from a sharp increase of cumulative daily precipitation (Figure 2A). Less than 10% of the annual precipitation occurred after April but before the fall wet season each year.

Snow started accumulating in November or December and attained a maximum depth in early spring at all stations (Figure 2B). The maximum depth occurred at the Upper Bull meteorological station, with 266, 380, 397 and 210 cm on 1 March in 2004, 24 March in 2005, 5 April in 2006 and 28 February in 2007, respectively. The maximum depth at other stations was less than 70% of those at the Upper Bull station. Snow depth declined almost monotonically as snow started melting. The snowpack was depleted 2–3 months after the maximum accumulation at the Upper Bul, but 4–6 weeks earlier at the other stations.

After maximum snow accumulation, streamflow runoff increased rapidly at all catchments, particularly in the relatively wet years 2005 and 2006 (Figure 2C). After snowpack depletion, cumulative runoff increased slightly with time. The annual runoff was much higher in 2005 and 2006, than in 2004 and 2007, at all catchments. The annual runoff also varied significantly among catchments, usually higher at B203 and B204 and lower at P303 and D102. For example, annual runoff was 38 and 12 cm at B203 and P303 in 2004 and 130 and 60 cm in 2005 at the same catchments, respectively. Streamflow discharge peaked 2–4 weeks earlier at the Providence than at the Bull catchments during the snowmelt period, i.e. from the times of maximum snow depth to snow depletion (bottom panels of Figure 3). Isolated streamflow peaks also occurred during winter and spring before the maximum snow accumulation, with some peak discharges even higher than those during the snowmelt period.

Ionic concentrations

Mean ionic concentrations of Ca^{2+}, Mg^{2+}, Na^{+} and K^{+} in streamflow were significantly higher at the Providence than at the Bull catchments (Table II). Mean concentrations of Ca^{2+} were greater than 200 $\mu eq\,l^{-1}$ ($1\sigma > 50\,\mu eq\,l^{-1}$) at the Providence catchments, but less than 160 $\mu eq\,l^{-1}$ ($1\sigma < 35\,\mu eq\,l^{-1}$) at the Bull catchments. Mean Cl^{-} concentrations were slightly higher at the Providence than at the Bull catchments, but SO_4^{2-} concentrations were slightly lower.

The temporal variation of ionic concentrations generally followed the opposite pattern of streamflow discharge, with lower concentrations at higher flows during

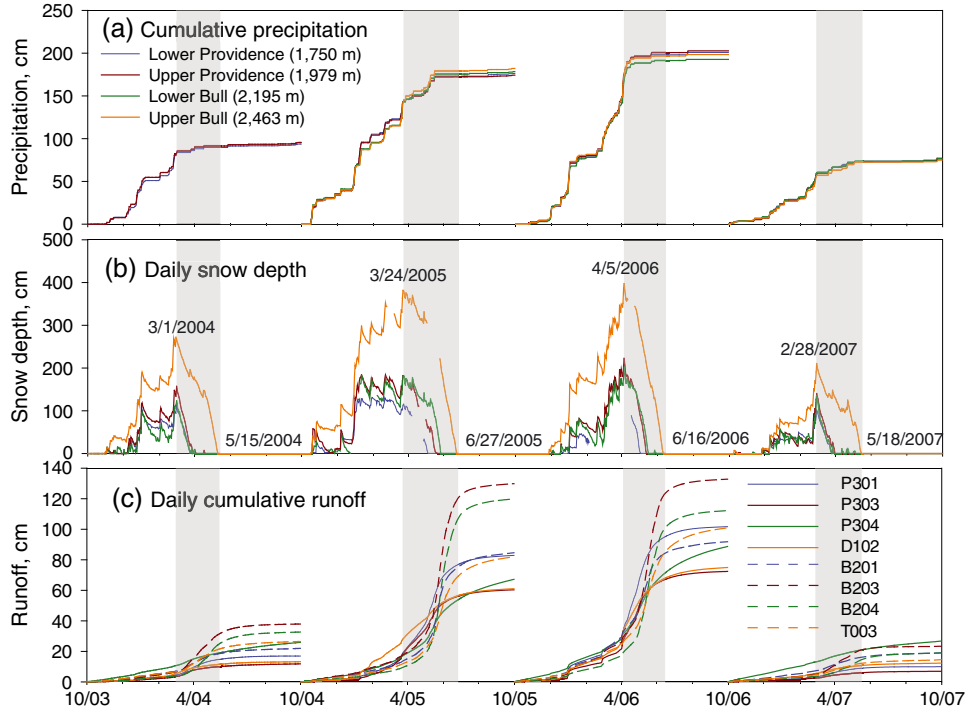

Figure 2. Hydrometeological data from water years 2004 to 2007 for (a) daily cumulative precipitation at four meteorological stations, (b) daily snow depth at the same stations, with peak and snow depletion dates at the Upper Bull station indicated and (c) daily cumulative runoff at eight catchments. Grey highlighted periods are from peak snow depth to snow depletion at the Upper Bull station

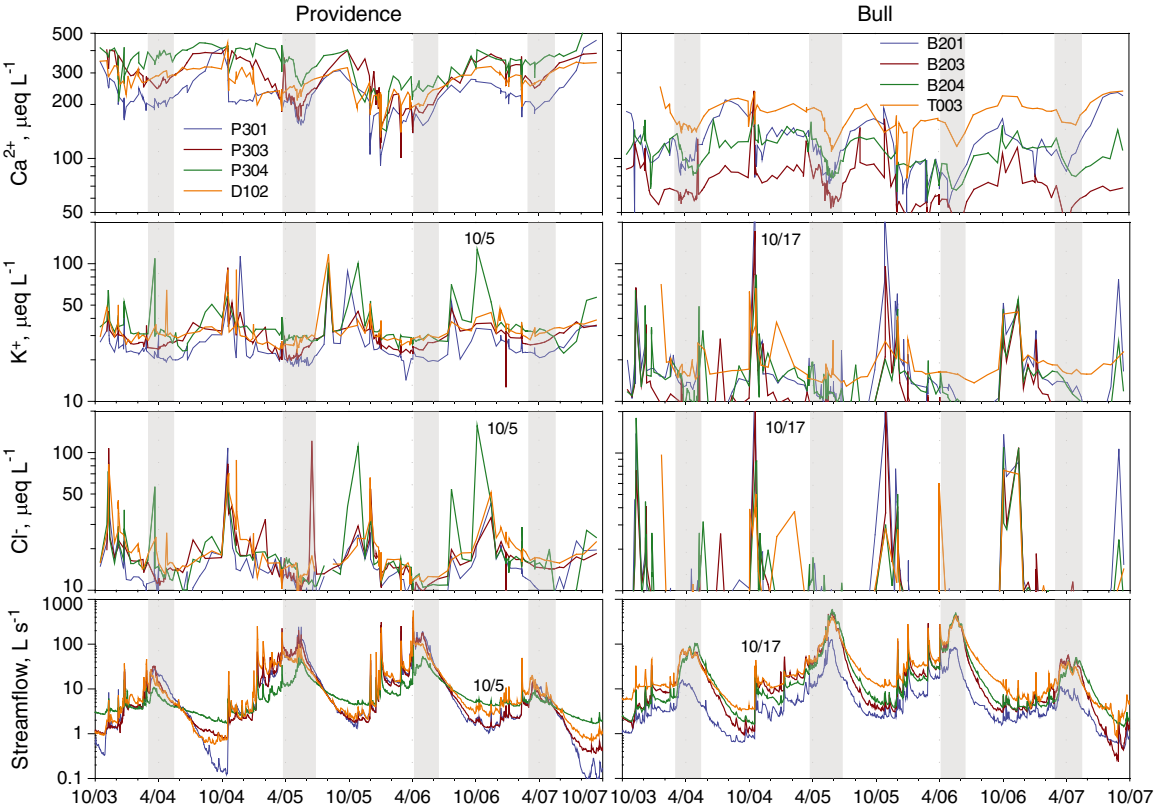

Figure 3. Concentrations of selected ions from water years 2004 to 2007 in streamflow at eight catchments in Providence and Bull, along with streamflow discharge, all in common logarithmic scales. Data points appear too intense, and thus, symbols are not used for clarity. Date-marked peaks were discussed in text. Grey highlighted periods are from peak snow depth to snow depletion at the Upper Bull station

snowmelt and higher concentrations at low discharges, as demonstrated by Ca^{2+}, K^+ and Cl^- in Figure 3. However, isolated peaks of high ionic concentrations, particularly those of K^+ and Cl^-, occurred following a transient increase in streamflow discharge during late summer and fall or even in winter (Figure 3). In contrast, spring rain storms did not show these isolated peaks in ionic concentrations. At the Providence catchments, ionic concentrations were generally lowest at P301 and highest at P304; at Bull, ionic concentrations were lowest at B203 and highest at T003, particularly for Ca^{2+} (Figure 3).

Mean ionic concentrations in snowmelt were much lower than in streamflow at both Providence and Bull catchments, but those in soil water were higher than in streamflow for all ions except Na^+ and SO_4^{2-} (Table II). The mean concentration of Ca^{2+} in snowmelt was 27 $\mu eq\,l^{-1}$, about 10% of that in streamflow at the Providence catchments, while that of soil water was 398 $\mu eq\,l^{-1}$, at least 20% higher than that in streamflow. The mean concentration of Na^+ in soil water was 16 $\mu eq\,l^{-1}$, twice that in snowmelt, but much lower than that in streamflow (45–171 $\mu eq\,l^{-1}$). Ionic concentrations in soil water varied significantly over time and locations, with 1σ values close to or greater than the mean values (Table II).

Mean ionic concentrations in meadow soil water and the B201 spring were greater than those in snowmelt but lower than those in streamflow (Table II). For instance, the mean concentration of Ca^{2+} was 81 $\mu eq\,l^{-1}$ at a meadow piezometer at B201, three times that in snowmelt, but about 30% of that in streamflow. Mean ionic concentrations in groundwater wells varied significantly; for example, Ca^{2+} was 426 $\mu eq\,l^{-1}$ in a well at Dinkey Creek Ranger Station and 1124 $\mu eq\,l^{-1}$ in a well at Blue Canyon Work Center (Table II).

Conservative tracers and number of endmembers

Streamflow chemical data were grouped into Providence and Bull datasets in order to determine conservative tracers and the number of endmembers by using DTMM. The distribution of the residuals between measured and projected values over the measured ionic concentrations indicated that a two-dimensional (2-D) mixing space was needed for the conservative mixing of streamflow chemistry at both Providence and Bull catchments (Figure 4). Ca^{2+}, Mg^{2+}, K^+, Cl^- and ANC were found to be conservative in streams at both sites. The R^2 values of the residual distributions were significantly lower for 2-D than 1-D for Ca^{2+}, K^+, Cl^- and ANC. For example, the R^2 values of Cl^- were 0.71 and 0.18 for 1-D *versus* 2-D at the Providence catchments; the respective values were 0.58 and 0.08 for Bull catchments. The residuals of SO_4^{2-} in 2-D showed a linear relationship with the measured ionic concentrations ($R^2 = 0.31$ at the Providence catchments, and 0.54 at the Bull catchments). Even though the R^2 values in 2-D were much lower for Na^+ than for SO_4^{2-}, 0.25 and 0.13 at the Providence and Bull catchments, respectively, the pattern of the Na^+ residual distributions and the residual magnitudes did not change much from 1-D to 2-D, indicating that Na^+, similar to SO_4^{2-}, did not behave completely conservative upon

Table II. Mean ionic concentrations (±1σ) in streamflow, snowmelt, soil water, spring water and groundwater

Sample location	Sample type	Number of samples	pH	EC ($\mu S\ cm^{-1}$)	ANC ($\mu eq\ l^{-1}$)	Ca^{2+} ($\mu eq\ l^{-1}$)	Mg^{2+} ($\mu eq\ l^{-1}$)	Na^{+} ($\mu eq\ l^{-1}$)	K^{+} ($\mu eq\ l^{-1}$)	Cl^{-} ($\mu eq\ l^{-1}$)	SO_4^{2-} ($\mu eq\ l^{-1}$)
P301	Streamflow	193	7.2 (0.3)	31 (10)	371 (73)	210 (50)	44 (10)	114 (22)	25 (10)	16 (14)	4 (2)
P303	Streamflow	183	7.3 (0.5)	44 (11)	461 (115)	259 (73)	67 (18)	132 (33)	29 (8)	17 (12)	5 (2)
P304	Streamflow	163	7.6 (0.4)	52 (19)	578 (107)	325 (75)	85 (16)	161 (27)	35 (12)	19 (14)	5 (2)
D102	Streamflow	187	7.5 (0.4)	41 (14)	487 (91)	255 (51)	56 (10)	171 (35)	33 (13)	21 (13)	4 (1)
B201	Streamflow	176	6.7 (0.3)	17 (6)	184 (43)	105 (35)	25 (11)	56 (16)	21 (34)	20 (52)	5 (2)
B203	Streamflow	167	6.8 (0.4)	14 (18)	132 (28)	74 (26)	21 (9)	45 (15)	15 (21)	15 (31)	6 (4)
B204	Streamflow	164	6.9 (0.3)	16 (5)	176 (25)	105 (24)	23 (4)	55 (14)	17 (12)	13 (18)	8 (5)
T003	Streamflow	109	7.1 (0.3)	27 (9)	266 (55)	159 (33)	32 (6)	70 (15)	21 (11)	10 (9)	7 (2)
Met stations	Snowmelt	83	5.5 (0.3)	9 (5)	39 (19)	27 (12)	7 (3)	8 (9)	8 (8)	4 (3)	5 (3)
Prenarts	Soil water	801	6.9 (0.7)	62 (59)	676 (584)	398 (264)	100 (62)	16 (9)	190 (337)	23 (95)	6 (5)
Piezometer B201	Meadow soil water	1		21	190	81	15	90	19	11	4
Piezometer P301	Meadow soil water	1		50	562	271	33	231	38	9	1
Spring B201	Spring water	1		16	128	50	8	72	17	11	8
Dinkey Creek tank	Groundwater	1		35	378	190	19	168	18	11	2
Dinkey Creek well	Groundwater	3		60 (18)	649 (190)	426 (193)	30 (7)	186 (5)	24 (3)	10 (1)	2 (0)
Glen Meadow well	Groundwater	3		31 (0)	350 (67)	139 (31)	11 (4)	212 (36)	9 (1)	12 (2)	3 (1)
Pacific Gas & Energy well	Groundwater	1		218	1314	541	13	2096	31	972	339
Blue Canyon well	Groundwater	2		303 (8)	1321 (323)	1124 (432)	111 (42)	1915 (74)	40 (4)	1416 (10)	433 (6)

mixing. It is thus deemed that concentrations of Ca^{2+}, Mg^{2+}, K^{+}, Cl^{-} and ANC in the streamflow were primarily caused by a mixing of three endmembers.

The same analysis was also performed for each individual catchment by using their own chemical data in the streamflow (data not shown). Conservative tracers and the number of endmembers of all individual catchments were consistent with the previous results. Note that NO_3^{-} and PO_4^{3-} were not included in previous analysis because their concentrations were below the analytical detection limits for a considerable portion of the samples. The DTMM requires that all species have measured values for all samples included in the analysis. Note also that the slopes of linear regressions for the distributions of residuals over the measured values had the same magnitude as the R^2 values, because the eigenvectors used to project the chemical concentrations in the streamflow were extracted using the chemical concentrations in the streamflow standardized to be zero mean and unit standard deviation.

Identification of endmembers for endmember mixing analysis

Mixing diagrams were constructed using the first two PCA projections with which eigenvectors were extracted from the correlations of four conservative tracers, Ca^{2+}, Mg^{2+}, K^{+} and Cl^{-} in the streamflow at both the Providence and Bull catchments (Figures 5 and 6), following Christophersen and Hooper (1992), Liu *et al.* (2004, 2008a, b) and Frisbee *et al.* (2011). All potential endmembers were also projected using the same eigenvectors as for the streamflow. ANC was not used in the analysis because it was calculated as the difference between the total cationic and anionic concentrations, and its precision and accuracy could not be quantitatively evaluated.

Most streamflow samples at both the Providence and Bull catchments are lined up in the mixing diagrams along an axis, with values for the streamflow samples collected during the snowmelt period close to values for the snowmelt collected at meteorological stations and with values for the streamflow samples collected in fall lying closer to the subsurface flow end of the axis (Figures 5 and 6). Thus, snowmelt runoff and subsurface flow were apparently two major endmembers contributing to streamflow. The streamflow samples scattered to the lower-right of the axis were also collected in fall. They were collected during storms and, essentially, those samples with isolated peaks of ionic concentrations in Figure 3. For example, the collection of streamflow samples on 17 October 2004 and 5 October 2006 (marked in Figure 3) occurred right after a storm of ~5.0 and 1.0 cm. The third endmember was thus a fall storm runoff.

Snowmelt runoff was characterized by ionic concentrations in snowmelt for all catchments at both Providence and Bull (Figures 5 and 6). Snowmelt is well positioned as a vertex to form a potential triangle to bind most of the streamflow samples. The relative distances between the *S*-space and *U*-space for ionic concentrations in snowmelt are 10% to 70%. The distance values are much larger than those in the meadow piezometer and spring (Table III) but

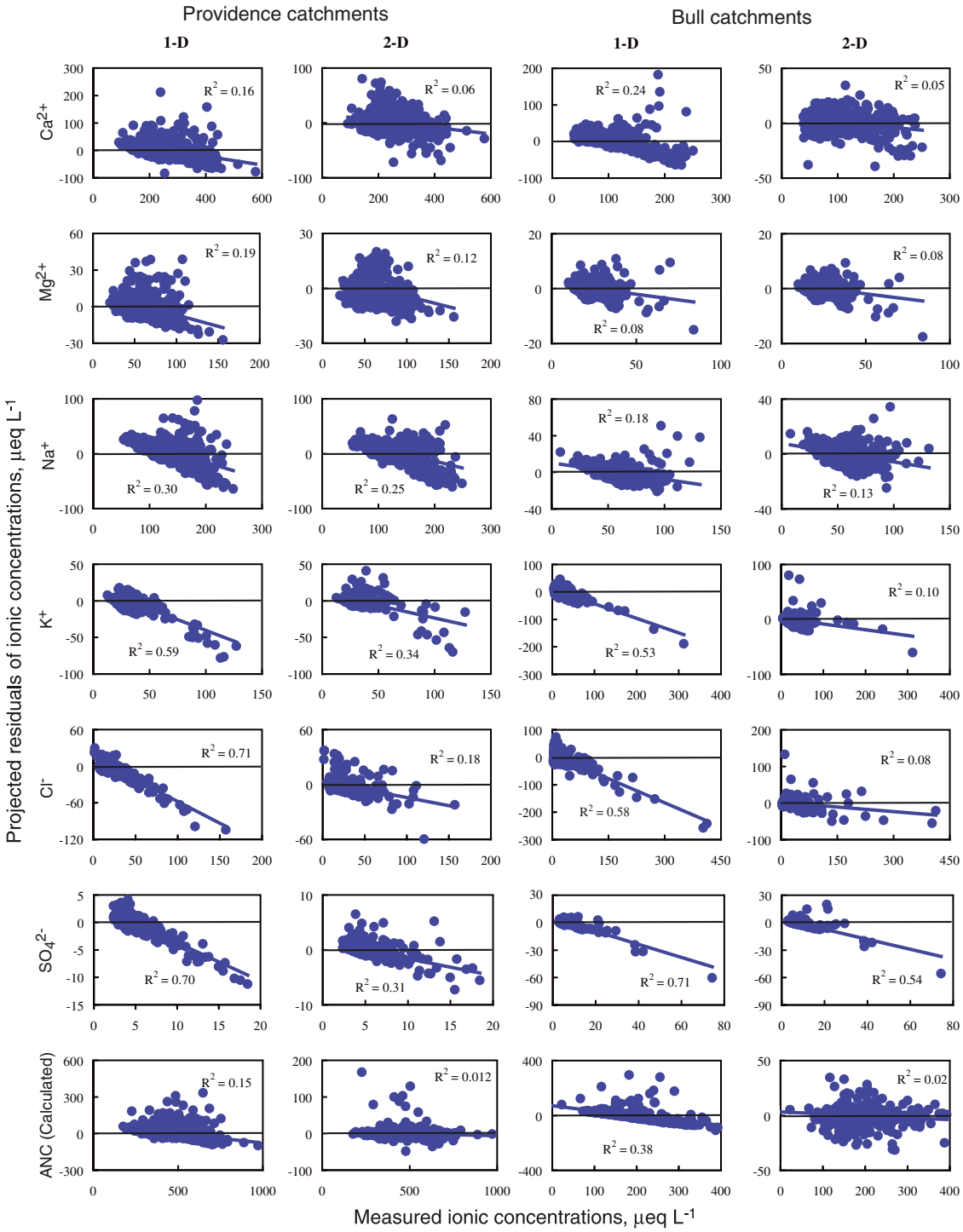

Figure 4. Distribution of residuals between projected and measured concentrations over measured concentrations in streamflow for all solutes used in the diagnostic tools of the mixing models in 1-D and 2-D mixing spaces

are comparable to the values reported for snowmelt elsewhere, e.g. for the Green Lake 4 catchment in the Rocky Mountains (Liu *et al.*, 2004) and the Valles Caldera in New Mexico (Liu *et al.*, 2008a). The large distances are primarily caused by lower ionic concentrations in snowmelt (Table II). Note that rain storms also occurred in spring when there was snow on the ground, and streamflow discharge responded spontaneously; but ionic concentrations did not respond with isolated peaks (Figures 2 and 3). Unlike rain storms in fall, rain on snow was chemically inseparable from snowmelt, and the runoff it generated was thus included as part of the snowmelt runoff.

A streamflow sample collected in the fall with the highest ionic concentrations was selected to characterize fall storm runoff, namely the one collected on 5 October 2006 at P304 for Providence catchments and on 17 October 2004 at B201 for the Bull catchments. The *U*-space and *S*-space distance was less than 5% and 10% for those two samples, respectively (Table III).

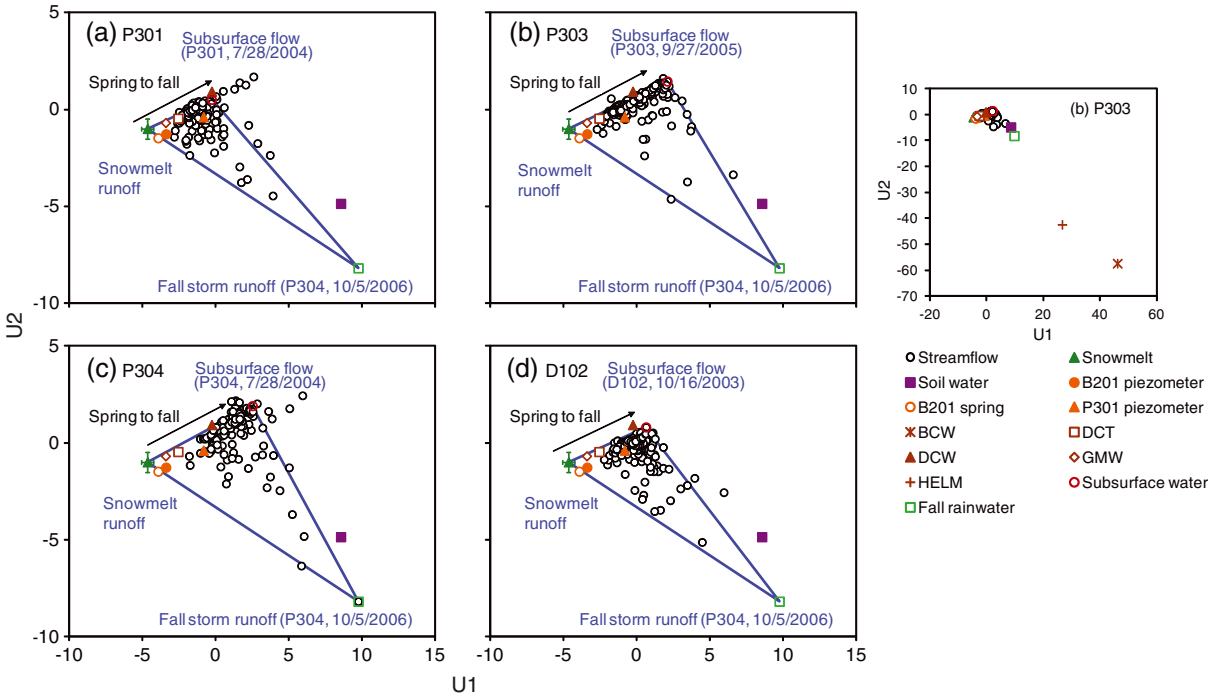

Figure 5. Mixing diagrams using the first two *U*-space projections, along with potential and selected endmembers and the triangle they form at Providence catchments. The ranges of ordinate and abscissa are focused on stream samples, with a smaller panel on the right showing full ranges at P303 as an example. Catchments and dates in parentheses under or beside the selected endmembers are streamflow samples used to characterize the endmembers (discussed in the text). BCW, for Black Canyon well; DCW, for a well near Dinkey Creek; DCT, for another well near Dinkey Creek (but sampled from a tank); GMW, for Glen meadow well; and HELM for the Pacific Gas and Energy well. For clarity of the figures, the errors are not shown for soil water and the Dinkey Creek well in the enlarged figures

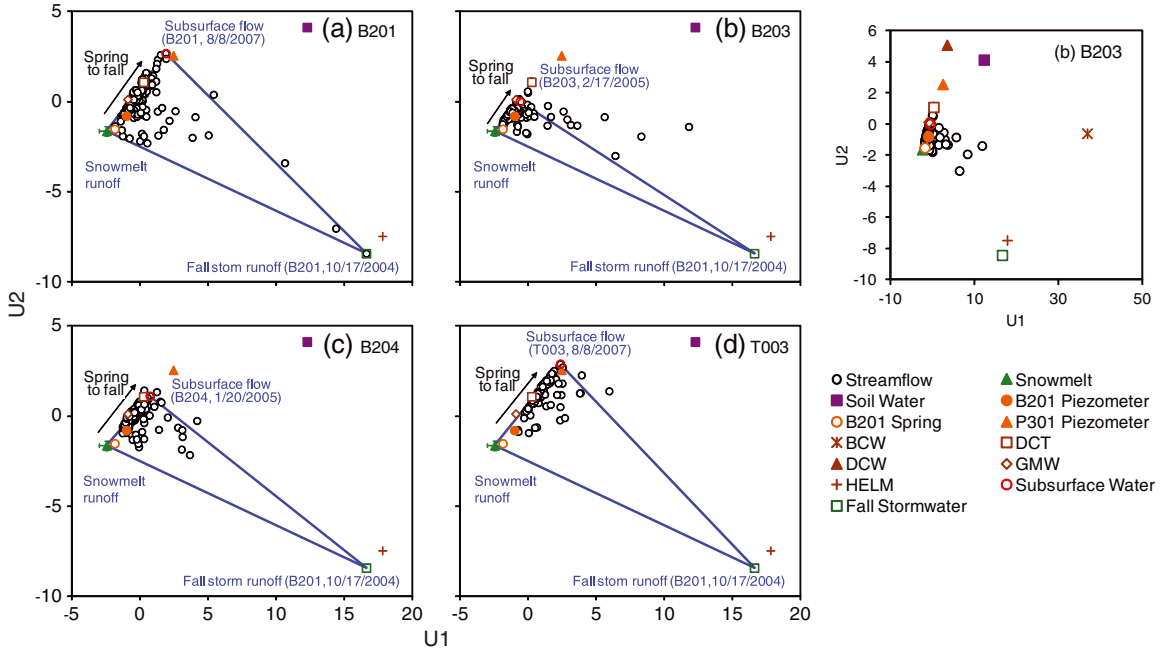

Figure 6. The same as Figure 5, except for the Bull catchments

Subsurface flow was characterized by streamflow samples collected during low discharges, following Liu *et al*. (2008a, b). The selection of streamflow samples for subsurface flow at each catchment in Table III was made on the basis of their geometrical positions in Figures 5 and 6 and the spatial endmember distances. The distances are usually less than 10% for all ions, except Cl^- (Table III). Similar to ionic concentrations in snowmelt, the large distances for Cl^- is likely caused by its relatively low concentrations (Table II).

Endmember contributions

Relative contributions of snowmelt runoff (% of streamflow) were less than 35% on average from 2004 to 2007 at the Providence catchments, with higher values (mean $\pm 1\sigma$ standard deviation) at P301 (33 ± 16) and

Table III. Mean spatial distance (1σ, if available) between *S*-space and *U*-space calculated by ionic concentrations and eigenvectors of ionic concentrations in streamflow for conservative tracers in potential endmembers. Note that the distance was normalized as percent of the measured ionic concentrations

Potential endmembers	Providence (%)				Bull (%)			
	Ca^{2+}	Mg^{2+}	K^{+}	Cl^{-}	Ca^{2+}	Mg^{2+}	K^{+}	Cl^{-}
Snowmelt	64 (15)	79 (12)	24 (21)	48 (36)	36 (11)	32 (15)	9 (5)	71 (43)
Soil water	33 (61)	29 (30)	40 (8)	758 (2975)	25 (27)	18 (15)	35 (12)	1206 (4073)
Piezometer B201	8	10	3	5	16	20	20	10
Piezometer P301	19	56	24	106	16	32	43	92
Spring B201	16	29	0	1	38	57	24	11
Dinkey Creek tank	23	63	8	16	24	58	37	73
Dinkey Creek well	38 (1)	205 (4)	13 (10)	37 (16)	29 (1)	135 (9)	90 (8)	287 (18)
Glen Meadow well	25 (7)	64 (53)	64 (3)	51 (1)	31 (4)	89 (55)	20 (12)	111 (13)
Pacific Gas and Energy well	101	66	1276	42	59	525	850	54
Blue Canyon well	73 (2)	10 (6)	1445 (183)	43 (0)	32 (12)	68 (88)	996 (46)	53 (4)
Streamflow samples collected during low flow as potential endmembers to characterize groundwater for each catchment								
P301 (7/28/2004)/B201 (8/8/2007)	8	11	1	1	4	6	9	53
P303 (9/27/2005)/B203 (2/17/2005)	1	0	3	6	6	6	24	18
P304 (7/28/2004)/B204 (1/20/2005)	3	3	2	4	2	2	2	22
D102 (10/16/2003)/T003 (8/8/2007)	9	12	3	6	0	0	7	33
Streamflow samples collected in the late fall as potential endmembers to characterize rainstorm runoff for the Providence and Bull catchments								
P304 (10/5/2006)/B201 (10/17/2004)	1	1	5	4	9	7	8	8

P303 (35 19) than at P304 (24 15) and D102 (26 14) (Table IV). The mean contributions of the subsurface flow varied between 60% and 70% at all of the Providence catchments, with 1σ standard deviations ranging from 17% to 20%. Fall storm runoff contributed less than 10% at all catchments. The Student's *t*-tests (two samples assuming unequal variances) showed that the mean contributions are not significantly different at P301 and P303 and at P304 and D102, respectively, for both snowmelt runoff and subsurface flow ($p > 0.05$ for two tails).

Snowmelt runoff contributed, on average, less than 40% of the streamflow from 2004 to 2007 at all Bull catchments except B201, with 32(21), 38(17) and 32 (16) at B203, B204 and T003, respectively (Table IV). The mean contribution of the snowmelt runoff was 56 (18)% at B201. The mean contributions of the subsurface flow varied between 60% and 66% for B203, B204 and T003, with 1σ standard deviations ranging from 16% to 20%, but 42(18)% for B201. Fall storm runoff contributed less than 4% on average at all catchments. The Student's *t*-tests showed that the mean contributions are not significantly different for B203 and T003 ($p > 0.05$ for two tails) for both snowmelt runoff and subsurface flow. More interestingly, the mean relative contributions of the snowmelt runoff and subsurface flow were not significantly different ($p > 0.05$) between some catchments across the Providence and Bull sites, including any pairs of B203, T003, P301 and P303 and between B204 and P303 (Figure 7).

Table IV. Mean relative (percent) endmember contributions (1σ) to streamflow from 2004 to 2007

Catchment	Streamflow ($l\,s^{-1}$)	Snowmelt runoff (%)	Fall storm runoff (%)	Subsurface flow (%)
P301	37	33 (16)	5 (8)	63 (18)
P303	51	35 (19)	4 (8)	61 (20)
P304	15	24 (15)	7 (13)	69 (20)
D102	40	26 (14)	8 (9)	66 (17)
B201	27	54 (18)	4 (11)	42 (18)
B203	86	32 (21)	3 (8)	65 (20)
B204	79	38 (17)	2 (4)	60 (17)
T003	90	32 (16)	2 (3)	66 (16)

Correlation of endmember contributions with streamflow

Contributions of snowmelt runoff and subsurface flow, by discharge magnitude rather than percent, were linearly correlated with the total streamflow discharge at both the Providence and Bull catchments (Figures 8 and 9). The R^2 values were 0.85–0.99 and 0.91–0.96 ($p < 0.001$) for snowmelt runoff and subsurface flow, respectively. The regression slopes varied from 0.45 to 0.75 for snowmelt runoff and from 0.25 to 0.53 for subsurface flow. The intercepts were all negative for the snowmelt runoff, with a magnitude equal to or less than 12, and all positive for subsurface flow, with a value less than 7.1. There were a few outliers for the subsurface flow in some of the catchments (Figure 9). These outliers mainly occurred on three days, 31 December in 2005, 2 January in 2006 and 28 February in 2006. It was presumably a result of analytical errors on ionic concentrations rather than instrumental errors on streamflow discharge, as there were no obvious outliers for snowmelt runoff.

DISCUSSION

Mechanism of streamflow generation across snow–rain transition

Streamflow was dominated by subsurface flow in these small, snow–rain transition zone catchments, with a mean relative contribution greater than 60% from 2004 to 2007,

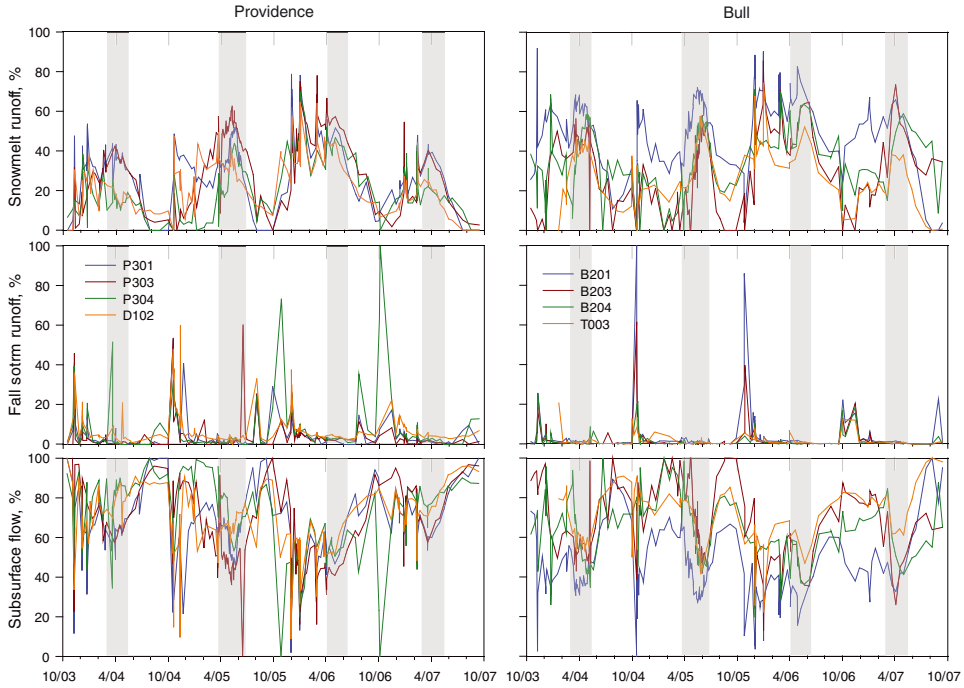

Figure 7. Relative (percent) endmember contributions to streamflow from water years 2004 to 2007 at the Providence and Bull catchments. Grey highlighted periods are from peak snow depth to snow depletion at the Upper Bull station

except for B201 (Table IV). The importance of the subsurface flow in streamflow generation is consistent with many studies from small, forested catchments in northern America with both snow-dominated and rain-dominated hydrology (e.g. Wilcox *et al.*, 1997; Newman *et al.*, 1998, 2004; Hogan and Blum, 2003; Tromp-van Meerveld and McDonnell, 2006). However, the contributions of subsurface flow to streamflow reported here are generally higher than those in the other reports. For example, subsurface flow accounted for only 40% of streamflow at the Hubbard Brook Experimental Forest (Hogan and Blum, 2003). Lateral subsurface flow occurred at an aspen-forested hillslope on the Boreal Plain only when precipitation is greater than 15 mm (Redding and Devito, 2008).

The contributions of the subsurface flow were highly correlated to streamflow discharge (Figure 9), indicating that subsurface water was rapidly delivered to streams in response to rainfall and snowmelt events. Soils at these catchments are dominated by sandy and loamy-sand textural classes, which are coarsely structured, with a sand fraction averaging above 0.70 (Bales *et al.*, 2011). This coarse soil structure may have resulted in the relatively high contributions of subsurface flow. The mean depth of soils from 87 soil pits is 75 and 77 cm for the Providence and Bull catchments, respectively (Johnson *et al.*, 2011). Thus, subsurface flow was most likely generated from the shallow soil–bedrock interface through preferential pathways, consistent with the mechanism reported by others for the Mediterranean and humid climates (e.g. Tromp-van Meerveld and McDonnell, 2006; Fiori *et al.*, 2007; Redding and Devito, 2010; Graham and Lin, 2011). On the other hand, soil-pit excavations indicate that soil thickness can vary from less than 50 cm to greater than 150 cm across short distances (Bales *et al.*, 2011). The bedrock is also highly weathered and consists of unconsolidated deep regolith, where hard bedrock is not typically encountered within a 150-cm depth (Bales *et al.*, 2011). These observations suggest that bedrock depressions or hollows may exist at these catchments and may play a significant role in regulating subsurface flow, as proposed for the Panola Mountain Research Watershed by Freer *et al.* (1997). Water infiltrating through preferential pathways, such as macropores, may have filled those hollows and then may have been released together with preevent water already stored in the hollows to streams, a 'fill and spill' mechanism suggested for the same Panola Mountain watershed by Tromp-van Meerveld and McDonnell (2006). We hypothesize that bedrock geomorphology at B201 is significantly different from the other catchments and that it is this difference that caused the lower percentage of subsurface flow at B201. However, confirming this hypothesis will depend on further data on bedrock geomorphology at these catchments.

Soil water in the unsaturated zone did not play a significant role in streamflow generation. Soil water was not identified as a contributing endmember, and its ionic concentrations were significantly different from those in the streamflow, piezometer and springs (Table II). Soil water chemistry of more than 800 samples was tested in EMMA by treating each individual sample as a potential endmember, but none of them qualified as a contributing endmember on the basis of their positions in the mixing diagrams and projected endmember distances (data not presented). The calculation of water balance at the watershed scale by Bales *et al.* (2011) showed that soil moisture equivalent to that stored above 1 m in depth is basically all consumed for evapotranspiration, consistent

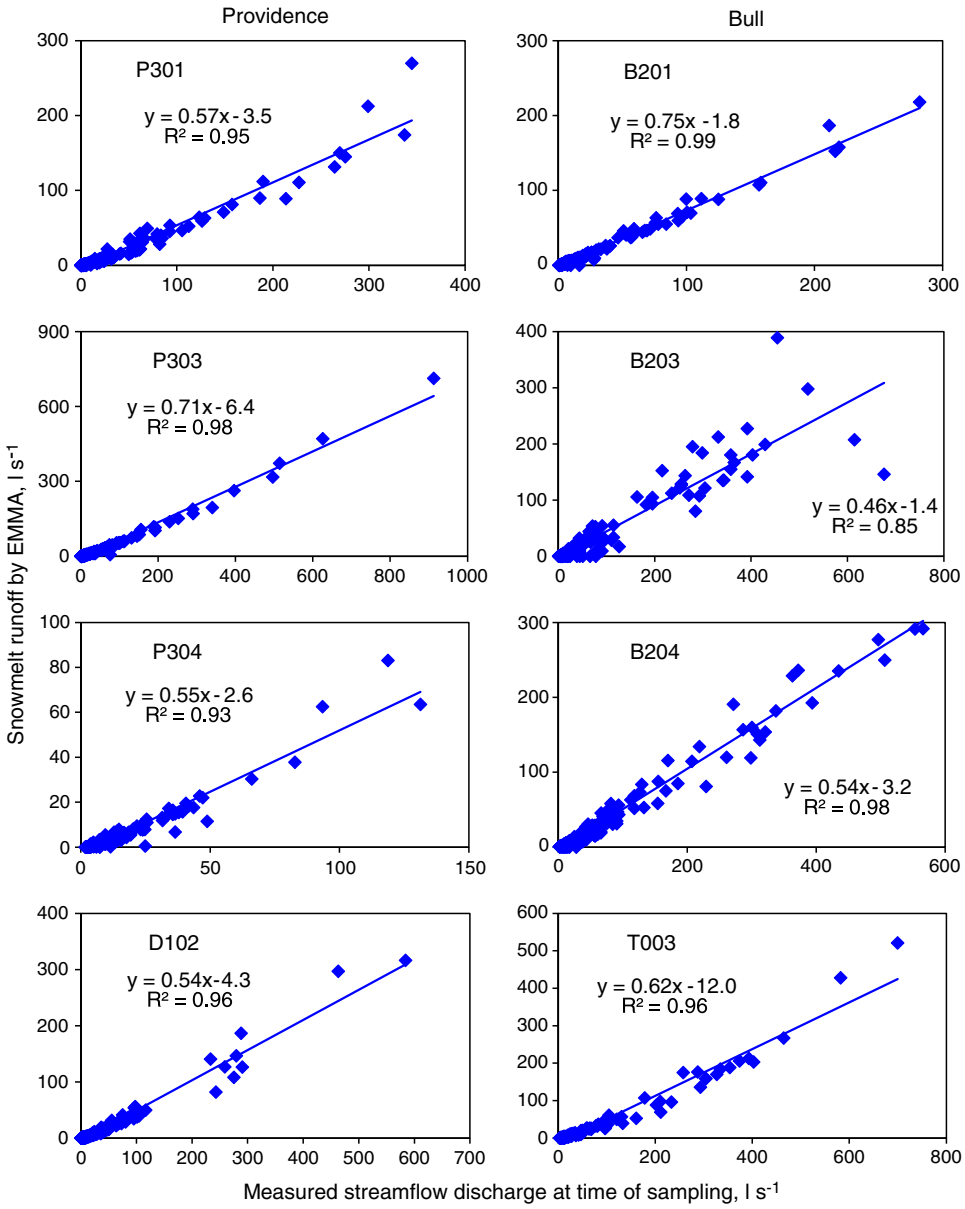

Figure 8. Correlation between snowmelt runoff and streamflow discharge at each catchment

with Barnard *et al.* (2010) for the H. J. Andrews Experimental Forest in Oregon. The volumetric water content of soil down to 1 m in depth varied between 20% and 30% during the snowmelt periods and below 10% after those periods. The high ionic concentrations in soil water were apparently caused by evapotranspiration. This argument is also consistent with a stable isotope study in an Oregon forest, where it was found that water entering the stream comes from preferential pathways and that soil water consumed by trees does not participate in translatory flow or significantly contribute to streamflow (Brooks *et al.*, 2009).

Also, different from a large watershed in the southern Rocky Mountains reported by Frisbee *et al.* (2011), these small catchments in southern Sierra Nevada were not fed by regional groundwater flow. Deep groundwater, such as those sampled in the Glen Meadow and the Blue Canyon well, was not a contributor to streamflow at these catchments (Figure 5).

Will a change in snow–rain ratio affect streamflow generation?

Streamflow generation was apparently not controlled by the proportion of snow *versus* rain at these catchments, as the mean relative contributions to streamflow were not significantly different between higher-elevation Bull and lower-elevation Providence catchments for both snowmelt runoff and subsurface flow (Figure 7). Thus, even if the snow–rain ratio at the higher-elevation Bull catchments decreases in the future because of climate warming, the mechanism of streamflow generation at the Bull catchments is not expected to change systematically or significantly. Note that the difference between this statement and statements regarding the timing of streamflow peaks in spring with declining snow in mountains. Less snow and earlier snowmelt have led to a shift in peak river runoff toward late winter and early spring in the US West (e.g. Barnett *et al.*, 2005; Stewart *et al.*, 2005) and at these eight

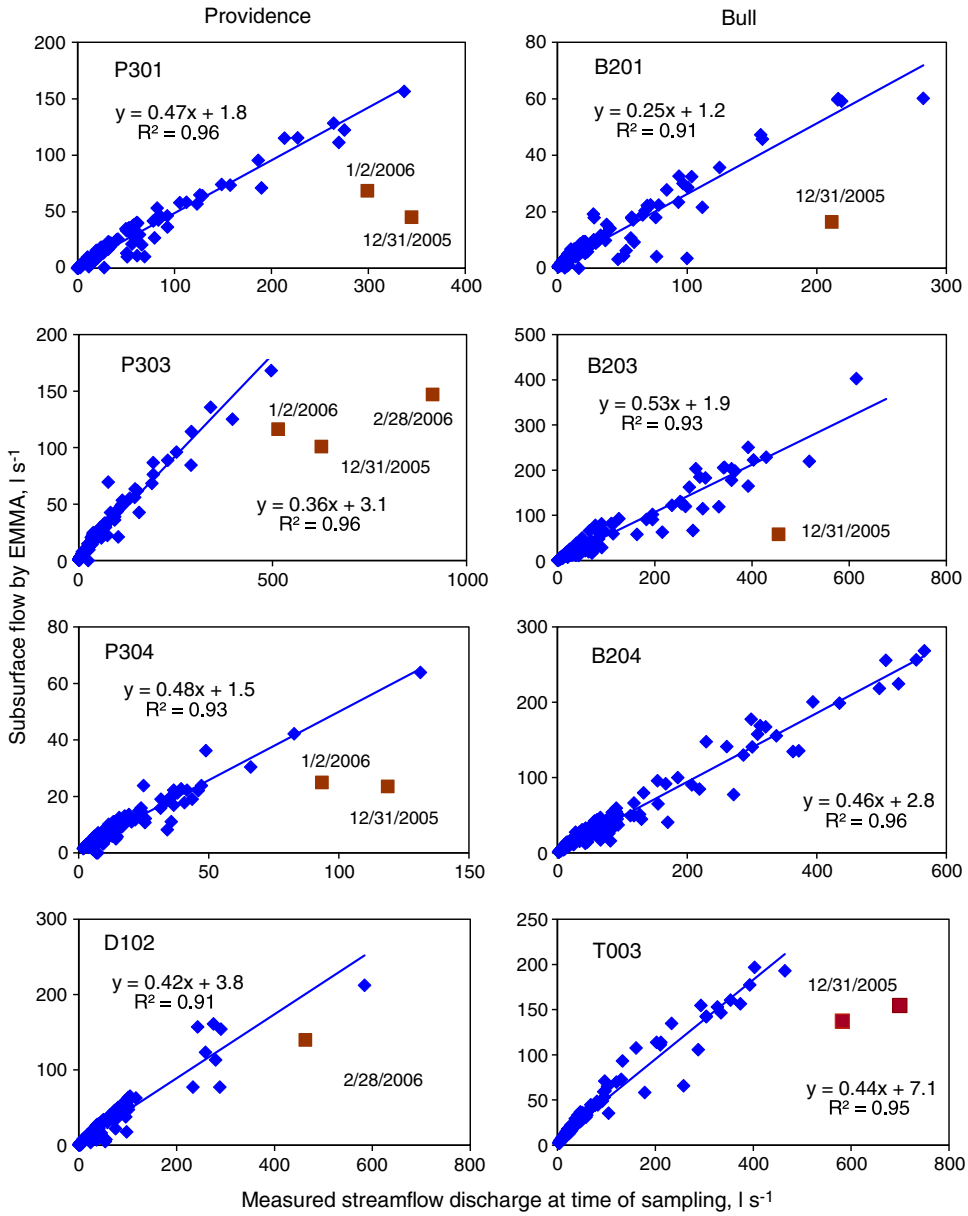

Figure 9. Correlation between subsurface flow and streamflow discharge at each catchment. Dark red squares are outliers

catchments (Hunsaker *et al*., 2012). Our argument here in this report means that even if, in a warmer climate, streamflow peaks earlier, the percent contributions of subsurface flow relative to snowmelt runoff (again which includes rain on snow) will not change significantly.

This result, however, was derived from these small, forested catchments located in a relatively narrow elevation range in Sierra Nevada. It is unclear how declines in the snow–rain proportion affect deep groundwater recharge or mountain-block recharge, as defined by Wilson and Guan (2004). As catchment size increases significantly, regional, long groundwater flowpaths may become increasingly important, as demonstrated by Frisbee *et al*. (2011), and streamflow regimes may change significantly with a change in the snow–rain ratio.

Also note that rain on snow was accounted the same way as snowmelt by the definition of snowmelt runoff in this study because they are chemically undistinguished. One might think that because rain on snow and snowmelt cannot be separated in the EMMA, the EMMA results would not support a robust examination of changes in streamflow generation associated with the snow–rain ratio. In fact, this is not correct. If rain on snow indeed generates different flowpaths from snowmelt, the responses of streamflow chemistry should be different. Say. if rain on snow would generate more subsurface flow than snowmelt, ionic concentrations in streamflow samples with rain on snow should be higher than those with snowmelt because ionic concentrations in subsurface water are higher. With higher ionic concentrations in streamflow having rain on snow, more subsurface flow contributions would be detected in EMMA even if the same chemical signatures are used for both rain on snow and snowmelt.

Evaluation of EMMA results

The selection of endmembers for both the Providence and Bull catchments and numerical solutions of EMMA were quantitatively evaluated by recreating streamflow

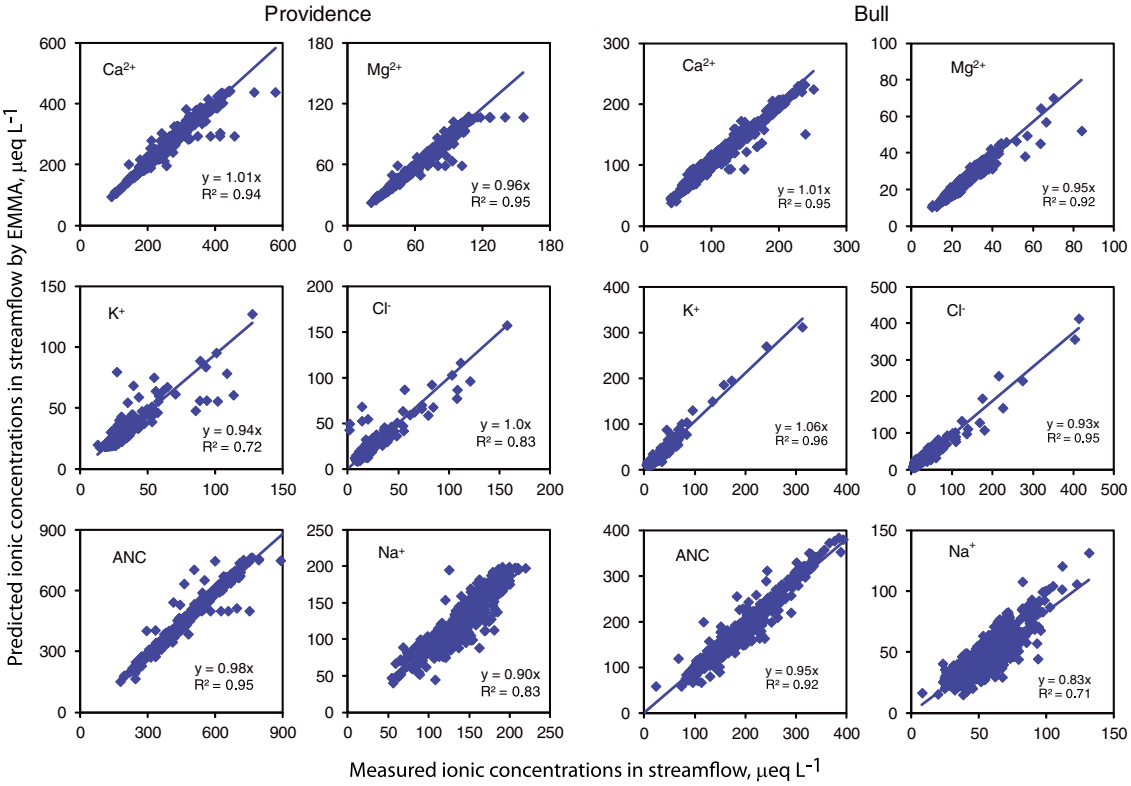

Figure 10. Recreation of ionic concentrations in streamflow on the basis of relative contributions of endmembers determined by endmember mixing analysis (EMMA) and ionic concentrations in endmembers. Note that acid neutralizing capacity (ANC) and Na^+ were not used in EMMA

chemistry using the products of relative contributions of EMMA and ionic concentrations of endmembers (Figure 10), following Christophersen and Hooper (1992) and Liu *et al.* (2004). This recreation is not self-recurring because the relative contributions of EMMA were determined by correlations of ionic concentrations rather than ionic concentrations themselves (Liu *et al.*, 2008a). The concentrations of Ca^{2+} and Mg^{2+} were very well recreated for both Providence and Bull catchments, with a slope near 1.0 and R^2 greater than 0.92 between measured and recreated values. The concentrations of K^+ and Cl^- were also very well recreated for Bull catchments, but R^2 values were much lower for Providence catchments. The lower R^2 values of K^+ and Cl^- at the Providence catchments were caused by a number of outliers. The ANC was reasonably well recreated for both Providence and Bull catchments, with a slope near 1.0 and $R^2 > 0.92$, even though it was not used in EMMA. The recreation of Na^+ was also reasonably good, with an R^2 of 0.83 and 0.71 for Providence and Bull catchments, respectively. Na^+ did not behave completely conservatively (Figure 4), and thus, an ideal recreation was not expected. Nonetheless, the recreation of streamflow chemistry enhanced the confidence of the endmember selection.

A single streamflow sample collected in October at P304 and B201 was used to characterize fall storm runoff for all Providence and Bull catchments, respectively (Figures 5 and 6). The sensitivity of the EMMA results to ionic concentrations of fall storm runoff was tested by replacing this sample by a stream sample collected in October at their own catchment (results not presented). It turns out that the EMMA results for all three endmembers are not very sensitive to ionic concentrations of fall storm runoff. The differences in relative contributions were less than 1% for snowmelt runoff and subsurface flow and less than 2% for fall storm runoff.

The geometrical position of soil water in the mixing diagram suggests that it could be a contributing endmember to streamflow instead of fall storm runoff at the Providence catchments (Figure 5). By using soil water rather than fall storm runoff in EMMA, the recreation of streamflow chemistry was very poor for K^+ and Cl^- at the Providence catchments, with an R^2 value of 0.55 and 0.44, respectively. This result is consistent with the large spatial distance projected for Cl^- using streamflow eigenvectors (Table III).

CONCLUSIONS

Streamflow is dominated by subsurface flow in small, forested, headwater catchments across the snow–rain transition elevations in the southern Sierra Nevada. Subsurface water is primarily formed by relatively rapid infiltration of snowmelt and rainwater to the interface of lower soil horizons and bedrock through preferential pathways, stored in hollows and delivered to streams by the 'fill and spill' mechanism. Both near-surface runoff and subsurface flow are very responsive to snowmelt and rainstorm events and are strongly linearly correlated with streamflow discharge. With changes in snow–rain proportions, systematic changes in the relative contributions of subsurface flow to snowmelt runoff (including rain on

snow) are not expected under current land use and vegetation coverage in the southern Sierra Nevada headwater catchments.

ACKNOWLEDGEMENTS

The authors appreciate the sample collection by T. Whitaker and other staff at Pacific Southwest Research Station, Forest Service, US Department of Agriculture (USDA), Fresno, California. This research was supported by the Forest Service, USDA; California's State Water Resources Control Board through Proposition 50 (the Water Security, Clean Drinking Water, Coastal, and Beach Protection Act of 2002); and the National Science Foundation (NSF), through the Southern Sierra Critical Zone Observatory (EAR-0725097) and grant BES-0610112 to the University of California, Merced. This research was also supported in part by an Evans–Allen project (225140) and a Capacity Building Grant (2011–02451), funded through the National Institute of Food and Agriculture (NIFA), USDA.

REFERENCES

Bales RC, Molotch NP, Painter TH, Dettinger MD, Rice R, Dozier J. 2006. Mountain hydrology of the western United States. *Water Resources Research* **42**: W08432. DOI: 10.1029/2005WR004387

Bales RC, Hopmans J, O'Geen T, Meadows M, Hartsough P, Kirchner P, Hunsaker C, Beaudette D. 2011. Soil moisture response to snowmelt and rainfall in a Sierra Nevada mixed-conifer forest. *Vadose Zone Journal* **10**: 786–799.

Barnard HR, Graham CB, Van Verselveld WJ, Brooks JR, Bond BJ, McDonnell JJ. 2010. Mechanistic assessment of hillslope transpiration controls of diel subsurface flow: a steady-state irrigation approach. *Ecohydrology* **3**: 133–142.

Barnett TP, Adam JC, Lettenmaier DP. 2005. Potential impacts of a warming climate on water availability in snow-dominated regions. *Nature* **438**. DOI: 10.1038, 17 November 2005.

Beighley RE, Dunne T, Melack JM. 2005. Understanding and modeling basin hydrology: interpreting the hydrogeological signature. *Hydrological Processes* **19**: 1333–1353. DOI: 10.1002/hyp.5567

Brooks JR, Barnard HR, Coulombe R, McDonnell JJ. 2009. Ecohydrologic separation of water between trees and streams in a Mediterranean climate. *Nature Geoscience*. DOI: 10.1038/NGE0722

Cayan DR, Kammerdiener SA, Dettinger MD, Caprio JM, Peterson DH. 2001. Changes in the onset of spring in the western United States. *Bulletin of the American Meteorological Society* **82**(3): 399–415.

Christophersen N, Hooper RP. 1992. Multivariate analysis of streamflow chemical data: the use of principal components analysis for the end-member mixing problem. *Water Resources Research* **28**(1): 99–107.

Dahlgren RA, Boettinger JL, Huntington GL, Amundson RG. 1997. Soil development along an elevational transect in the western Sierra Nevada, California. *Geoderma* **78**: 207–236.

Dore MHI. 2005. Climate change and changes in global precipitation patterns: What do we know? *Environmental International* **31**: 1167–1181.

Fiori A, Rommanelli M, Cavalli DJ, Russo D. 2007. Numerical experiments of streamflow generation in steep catchments. *Journal of Hydrology* **339**: 183–192.

Freer J, McDonnell JJ, Beven KJ, Brammer DD, Burn D, Hooper RP, Kendall C. 1997. Topographic controls on subsurface storm flow at the hillslope scale for two hydrologically distinct small catchments. *Hydrological Processes* **11**(9): 1347–1352.

Frisbee MD, Phillips FM, Campbell AR, Liu F, Sanchez SA. 2011. Streamflow generation in a large, alpine watershed in the southern Rocky Mountains of Colorado: Is streamflow generation simply the aggregation of hillslope runoff responses? *Water Resources Research* **47**: W06512. DOI: 10.1029/2010WR009391

Giger DR, Schmitt GJ. 1993. Soil Survey of Sierra National Forest, USDA-SCS, U. S. Gov. Print. Off, Washington, DC.

Graham CB, Lin HS. 2011. Controls and frequency of preferential flow occurrence: a 175-event analysis. *Vadose Zone Journal* **10**(3): 816–831.

Hogan JF, Blum JD. 2003. Tracing hydrologic flow paths in a small forested watershed using variations in $^{87}Sr/^{86}Sr$, [Ca]/[Sr], [Ba]/[Sr] and $\delta^{18}O$. *Water Resources Research* **39**(10): 1282. DOI: 10.1029/2002WR001856

Hooper RP. 2003. Diagnostic tools for mixing models of streamflow chemistry. *Water Resources Research* **39**(3): 1055. DOI: 10.1029/2002WR001528

Hunsaker C, Whitaker T, Bales RC. 2012. Water yield and runoff timing across the rain-snow transition in California's southern Sierra Nevada. *Journal of the American Water Resources Association* (JAWRA) 1–12. DOI: 10.1111/j.1752-1688.2012.00641.x

Intergovernmental Panel on Climate Change (IPCC). 2007. In *Climate Change 2007: The Physical Science Basis. Contribution of Working Group I to the Fourth Assessment Report of the Intergovernmental Panel on Climate Change*, Solomon S *et al*. (eds). Cambridge University Press: New York.

Johnson DW, Hunsaker CT, Glass DW, Rau BM, Roath BA. 2011. Carbon and nutrient contents in soils from the Kings River Experimental Watersheds, Sierra Nevada Mountains, California. *Geoderma*. DOI: 10.1016/j.geoderma.2010.10.019

Knowles N, Dettinger MD, Cayan DR. 2006. Trends in snowfall versus rainfall in the Western United States. *Journal of Climate* **19**: 4545–4559.

Kundzewicz ZW, Mata LJ, Arnell NW, Döll P, Kabat P, Jiménez B, Miller KA, Oki T, Sen Z, Shiklomanov IA. 2007. Freshwater resources and their management. In *Climate Change 2007: Impacts, Adaptation and Vulnerability, Contribution of Working Group II to the Fourth Assessment Report of the Intergovernmental Panel on Climate Change*, Parry ML, Canziani OF, Palutikof JP, van der Linden PJ, Hanson CE (eds). Cambridge University Press: Cambridge, UK; 173–210.

Liu F, Williams MW, Caine N. 2004. Source waters and flow paths in an alpine catchment, Colorado Front Range, USA. *Water Resources Research* **40**: W09401. DOI: 10.1029/2004WR003076

Liu F, Bales RC, Conklin MH, Conrad ME. 2008a. Streamflow generation from snowmelt in semi-arid, forested and seasonally snow-covered catchments, Valles Caldera, New Mexico. *Water Resources Research* **44**: W12443. DOI: 10.1029/2007WR006278

Liu F, Parmenter R, Brooks P, Conklin MH, Bales RC. 2008b. Intra- and inter-annual variation of streamflow pathways in semiarid, forested catchments, Valles Caldera, New Mexico. *Ecohydrology* **1**(3): 239–252. DOI: 10.1002/eco.22

McNamara JP, Chandler D, Seyfried M, Achet S. 2005. Soil moisture states, lateral flow, and streamflow generation in a semi-arid, snowmelt-driven catchment. *Hydrological Processes* **19**: 4023–4038.

Mote PW Hamlet AM, Clark MP, Lettenmaier DP. 2005. Declining mountain snowpack in western North America. *Bulletin of the American Meteorological Society* **86**: 1–39.

Newman BD, Campbell AR, Wilcox BP. 1998. Lateral subsurface flow pathways in a semiarid ponderosa pine hillslope. *Water Resources Research* **34**(12): 3485–3496.

Newman BD, Wilcox BP, Graham RC. 2004. Snowmelt-driven macropore flow and soil saturation in a semiarid forest. *Hydrological Processes* **18**: 1035–1042.

Rauscher SA, Pal JS, Diffenbaugh NS, Benedetti MM. 2008. Future changes in snowmelt-driven runoff timing over the western US. *Geophysical Research Letters* **35**: L16703. DOI: 10.1029/2008GL034424

Redding T, Devito K. 2008. Lateral and vertical flow thresholds for aspen forested hillslopes on the Western Boreal Plain, Alberta, Canada. *Hydrological Processes* **23**: 4287–34300

Redding T, Devito K. 2010. Mechanisms and pathways of lateral flow on aspen-forested, Luvisolic soils, Western Boreal Plains, Alberta, Canada. *Hydrological Processes* **24**: 2995–3010. DOI: 10.1002/hyp.7710.

Rice KC, Hornberger GM. 1998. Comparison of hydrochemical tracers to estimate source contributions to peak flow in a small, forested, headwater catchment. *Water Resources Research* **34**(7): 1755–1766.

Stewart IT, Cayan DR, Dettinger MD. 2004. Changes in snowmelt runoff timing in western North America under a 'business as usual' climate change scenario. *Climatic Change* **62**: 217–232.

Stewart IT, Cayan DR, Dettinger MD. 2005. Changes toward earlier streamflow timing across western North America. *Journal of Climate* **18**: 1136–1155.

Tromp-van Meerveld HJ, McDonnell JJ. 2006. Threshold relations in subsurface stormflow: 1. A 147-storm analysis of the Panola hillslope. *Water Resources Research* **42**: W02410. DOI: 10.1029/2004WR003778

Wilcox BP, Newman BD, Brandes D, Davenport DW, Reid K. 1997. Runoff from a semiarid ponderosa pine hillslope in New Mexico. *Water Resources Research* **33**(10): 2301–2314.

Wilson JL, Guan HD. 2004. Mountain-block hydrology and mountain-block recharge. In *Groundwater Recharge in A Desert Environment: the Southwestern United States*, Phillips FM, Hogan JF, Scanlon BR (eds). AGU: Washington, DC.

